

Reduction of base-collector capacitance in GaInAs/InP heterojunction bipolar transistor by using InP buried growth of tungsten

Y. Miyamoto, T. Arai, Y. Harada, S. Yamagami and K. Furuya

Department of Physical Electronics, Tokyo Institute of Technology,

We report a novel approach to improve the performance of InP-based heterojunction bipolar transistors (HBTs). A buried-metal heterojunction bipolar transistor (BM-HBT), where tungsten stripes with a same area as an emitter metal were buried by an i-InP collector layer, was fabricated to realize a reduction in a total base-collector capacitance (C_{BCT}). C_{BCT} calculated from S-parameter measurement was about 20 % of that of conventional HBT and the reduction of C_{BCT} was confirmed.

Introduction

In heterojunction bipolar transistors (HBTs), reduction of total base-collector capacitance (C_{BCT}) is effective in a improvement of high speed operation[1-3]. We proposed buried metal heterojunction bipolar transistor (BM-HBT), in which tungsten stripe with a same area of emitter is buried in InP collector layer, to eliminate extrinsic base collector capacitance[4].

Figure 1 shows the schematic view of BM-HBT. Metal wires with an area equal to that of the emitter mesa are formed on the semi-insulating InP substrate. These are buried in an i-InP layer at the growth of the HBT layers. The buried metal wires are in contact with the i-InP collector layer and operate as a Schottky collector electrode. There is no conductive layer under the extrinsic base region. Therefore, the reduction of C_{BCT} is achieved.

Figure 2 shows the calculated dependence on emitter width. In BM-HBT, maximum oscillation frequency (f_{MAX}) can be increased with decrease of emitter width without penalty of current gain cutoff frequency (f_T).

To fabricate BM-HBT, a key technology is a buried growth of metal and we studied the condition of the buried growth. By using the obtained conditions, BM-HBT with a few micron wide emitter was fabricated to show feasibility of BM-HBT.

InP buried growth of metal

The buried growth must satisfy the following requirements. The burying InP must be a single crystal. Hence, lateral overgrowth from the window region is essential. To fabricate base and emitter layers, the top surface must be flat. To reduce transit time, thinner overgrown layer is preferable. No formation of a void in the burying material is also required. The embedded metal should not form an alloy with the compound semiconductor at the growth temperature of organometallic vapor phase epitaxy (OMVPE). It was confirmed that tungsten

fulfilled this requirement[5,6]. Thus, we selected tungsten as the buried metal.

To find growth conditions, lateral growth on the tungsten stripe was observed by the cross-sectional shape after the growth of a 500-nm-thick InP layer. Four different stripe directions that were 0° , 30° , 45° and 90° from $\langle 011 \rangle$ direction were fabricated.

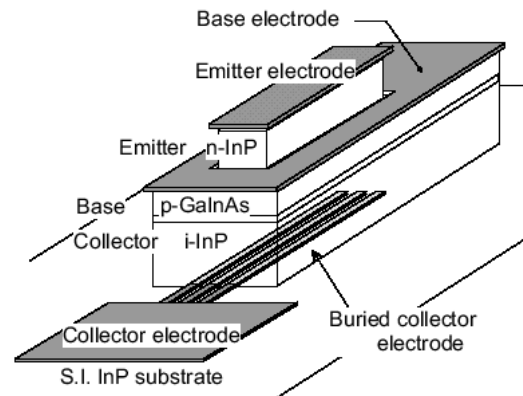


Fig. 1 Schematic view of BM-HBT

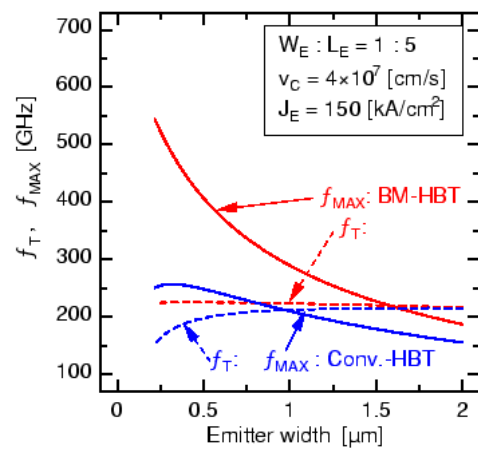


Fig. 2 Calculated f_T and f_{MAX} at BM-HBT and conventional HBT. When emitter width is reduced, BM-HBT provides higher f_{MAX} .

The pitch and width of the tungsten wires were 2 μm and 1 μm , respectively. In the OMVPE growth, trimethylindium and triethylgallium as group III materials, and phosphine and arsine as group V materials were used. The growth temperature, the growth rate and the V/III ratio were in the range of 550-650 $^{\circ}\text{C}$, 14-42 nm/min and 140-560, respectively. We paid attention to the facet angle and thickness/width ratio in the cross-section of the lateral grown region. To prevent the formation of a void, the facet of lateral growth must have an acutely angled facet. To be buried under a thinner layer, the ratio of thickness to width of a grown mesa in the window region was the figure of merit. Lower thickness/width ratio will realize buried growth with a thinner layer.

As a result, the growth temperature and growth rate had strong influence while AsH_3 flow rate had a little influence. Lowering growth temperature and increase of TMI flow rate were effective to reduce thickness/width ratio. However, excessive lowering of the temperature and excessive increase of the flow rate resulted in poly-crystal-like deposition. When the angle were 30 $^{\circ}$ and 45 $^{\circ}$, no void formation was observed.

To confirm embedding tungsten stripes by a flat layer, the thickness of InP was increased to 1.0 μm under optimized conditions. The growth temperature, V/III ratio and growth rate were 600 $^{\circ}\text{C}$, 460 and 28 nm/min, respectively. Moreover, the structure of DHBT was grown on the InP buried layer. Figure 3 shows a cross-sectional SEM view of tungsten stripes after the buried growth when the stripe direction was 45 $^{\circ}$. Complete embedding by a InP layer with flat top surface and no formation of voids was observed. When the stripe direction was 30 $^{\circ}$, we could not get flat hetero-interface, although no void formation was confirmed.

Fabrication of BM-HBT with a few micron wide emitter

In the calculation of the RF characteristics of BM-HBT, the estimated collector thickness for the highest f_{max} is about 300 nm[4]. Hence the width of the buried wires must be less than 300 nm. In the case of fabrication using a 2- μm -wide emitter applying a conventional process, many tungsten wires of fine width must be buried under the emitter.

We fabricated the devices with emitter widths of 2 μm and 3 μm . We initiated the fabrication process by forming tungsten stripes on the semi-insulating InP substrate by the metal-stencil liftoff process with electron beam lithography[7]. The total widths of the stripes were 2 μm and 3 μm . The width, thickness and length of the wires were 100 nm, 40 nm and 16 μm , respectively. The period of wires

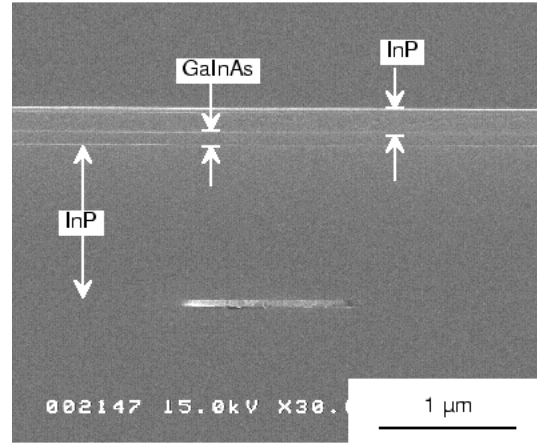


Fig. 3 Cross section of buried growth of InP using TMI. Tungsten width was 1 μm . Growth temperature was 600 $^{\circ}\text{C}$. After InP buried growth, DHBT structure without sub-collector layer was grown.

Layer	Material	Doping [cm^{-3}]	Thickness [nm]
Contact	n-GaInAs	2×10^{19}	20
Emitter	n-InP	2×10^{19}	70
	n-InP	5×10^{17}	100
Base	p-GaInAs	2×10^{17}	50
Collector	i-GaInAs	---	40
	i-GaInAsP	---	20
	n-InP	5×10^{17}	5
	i-InP	---	230

Table 1 Layer structure parameters of the fabricated BM-HBT.

was 200 nm. The stripes were oriented at an angle of 45 $^{\circ}$ from $\langle 01\bar{1} \rangle$. At the same time, a tungsten mark for alignment of the emitter with the buried tungsten stripes was formed. Next, DHBT structure without a subcollector layer was grown on the sample by OMVPE. The layer structure is shown in Table 1. The growth temperatures were 600 $^{\circ}\text{C}$, 500 $^{\circ}\text{C}$ and 565 $^{\circ}\text{C}$ for the collector layers, a base layer and emitter layers, respectively. The growth condition were equal to optimized condition as mentioned before. Next, the mesa structure was formed by wet chemical etching and patterned by photolithography. The InP layers were etched by a $\text{HCl}:\text{H}_3\text{PO}_4=1:1$

solution, while the GaInAs layers and the GaInAsP layer were etched by a citric acid:H₂O₂=5:1 solution. An emitter electrode was formed in alignment with the buried tungsten stripes. A base electrode was formed by a self-alignment technique. Areas of the emitter and base electrode were 2×10 μm² and 6×16 μm², respectively. The emitter and base metals were Ti/Pt/Au. The device was isolated by the formation of a base mesa. At the same time, a part of the buried tungsten stripes was exposed for connection and a collector electrode was formed on the stripes. Then the device was embedded by polyimide for planarization and passivation. After opening of the contact windows using reactive ion etching, Au/Cr were evaporated for interconnection.

Device characteristics and discussions

Figure 4 shows the common-emitter collector I-V characteristics of a device with a 2-μm-wide emitter. The current gain was about 70 at the collector voltage (V_c) of 4 V. Microwave S-parameters were measured from 50 MHz to 30 GHz using an HP8722 network analyzer. f_T and f_{max} were extrapolated from the -20 dB/decade regions of current gain ($|h_{21}|$) and Mason's unilateral gain (U), respectively. In the measurement of the dependence of f_T and f_{max} on collector current (I_c), the values of f_T and f_{max} reached peak points ($f_T = 33.5$ GHz, $f_{max} = 47.3$ GHz) at I_c = 4 mA and V_c = 6 V.

The C_{BCT} of 10.3 fF was calculated from the imaginary part of Y₁₂ parameters in a low-frequency region. We also fabricated a conventional HBT with almost the same planar dimensions as a reference. The measured C_{BCT} of the reference was 53 fF when the collector thickness was 260 nm. C_{BCT} values of BM-HBT and conventional HBT could not be compared with each other directly, because C_{BCT} depends on collector layer thickness and the buried growth had a possibility to change the thickness. To measure the collector layer thickness of fabricated devices, BM-HBT was cut by a focused ion beam. A cross-sectional SEM view of the fabricated device with emitter width of 3 μm is shown in Fig. 5. It was confirmed that the emitter mesa was aligned with the buried tungsten stripes and no void was formed around the buried tungsten. The measured collector thickness was 290 nm. The effective base-collector junction area (S_{BCJ}) was calculated from C_{BCT} considering the difference in the collector layer thickness. When we assumed two parallel plate model and complete depletion of the collector, S_{BCJ} of BM-HBT and conventional-HBT were calculated as 26 μm² and 119 μm², respectively. Thus, we achieved a BM-HBT in which the effective base-collector junction area was 22 % of that of conventional HBT.

The extrinsic emitter resistance (R_{EE}) of 15

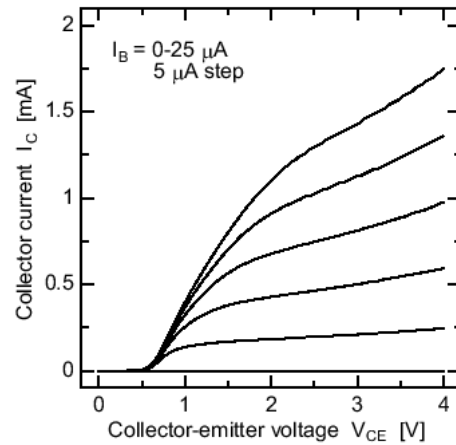


Fig. 4 Common-emitter collector I-V characteristics of BM-HBT with an emitter area of 2×10 μm².

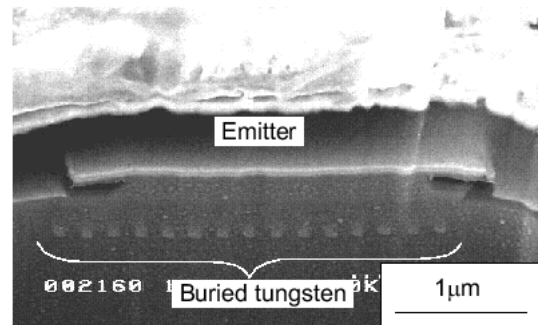


Fig. 5 A SEM view of a cross section cut by a focused ion beam. Measured collector thickness was 290 nm

was measured using the open collector method. However, the extrinsic collector resistance (R_{CC}) could not be measured using the open emitter method, because the interface between the collector layer and the collector metal formed a Schottky junction and the base-collector junction did not operate as a p-n diode. The value of R_{EE}+R_{CC} estimated from the linear region of the common-emitter collector I-V characteristics was about 400 Ω. As a result, estimated R_{CC} was very high.

Because the collector junction of BM-HBT was biased as a forward Schottky junction, contact resistance between collector layer and collector metal must be sufficiently small. Thus, we assumed that the high R_{CC} was due to the high resistivity of tungsten and we measured the resistance of wires with different lengths. The fabrication process was similar to that used for forming the buried tungsten stripes and interconnection in BM-HBT. The measured resistivity was 160 μΩ cm. The value of R_{CC} calculated using this resistivity was 360 Ω and

the reason for the high resistance could be explained. The resistivity of tungsten was strongly dependent on sample temperature at evaporation[8] and a value less than $10 \mu \text{ cm}$ was reported when the temperature was about 200°C [9]. In the fabrication process of BM-HBT, the sample holder was cooled to 0°C to prevent deformation of the resist pattern. Thus, optimization of the fabrication process will overcome the high resistivity of tungsten, resulting in high-speed operation of BM-HBT.

To exhibit superior characteristics of BM-HBT, narrower emitter is essential as show in Fig.2. By using electron beam lithography, we recently developed a fabrication process of InP DHBT with $0.5 \mu\text{m}$ wide emitter[10]. Thus next step is the combination of this process and BM-HBT.

Conclusion

The OMVPE growth conditions for buried growth of tungsten stripes was studied. Under optimized conditions, the ratio of grown InP thickness to buried tungsten width was about 1. By using the optimized conditions, GaInAs/InP-based BM-HBT with an emitter area of $2 \times 10 \mu\text{m}^2$ was successfully fabricated. S-parameters measurements indicated f_T of 33.5 GHz and f_{max} of 47.3 GHz at I_C of 4 mA. S_{BCJ} of BM-HBT was 22 % that of conventional HBT and the reduction of C_{BCT} was confirmed. This result showed the possibility of high performance of BM-HBT.

References

- [1] K. Kurishima: IEEE Trans. Electron Device, **43** (1996) 2074.
- [2] Y. Miyamoto, J. M. M. Rios, A. G. Dentai and S. Chandrasekhar: IEEE Electron Device Lett., **17** (1996) 97.
- [3] U. Bhattacharya, M. J. Mondry, G. Hurts, I.-H. Tan, R. Pallela, M. Reddy, J. Guthrie, M. J. W. Rodwell and J. E. Bowers: IEEE Electron Device Lett., **16** (1995) 357.
- [4] T. Arai, H. Tobita, Y. Harada, M. Suhara, Y. Miyamoto and K. Furuya: Proc. 11th Int. Conf. Indium Phosphide and Related Materials, Davos, (1999) p. 183.
- [5] H. Hongo, Y. Miyamoto, J. Suzuki, M. Funayama, T. Morita and K. Furuya: Jpn. J. Appl. Phys., **33** (1994) 925.
- [6] M. Suhara, L.-E. Wernersson, B. Gustafson, N. Carlsson, W. Seifert, A. Gustafsson, J.-O. Malm, A. Litwin, A. Samuelson and K. Furuya: Jpn. J. Appl. Phys., **38** (1999) 3466.
- [7] T. Arai, H. Tobita, Y. Harada, M. Suhara, Y. Miyamoto and K. Furuya: Physica E, **7**, (2000) 896
- [8] K. Y. Ahn: Thin Solid Films, **150** (1987) 469.

- [9] R. L. Krams, A. Berntsen and W. C. Sinke: Mat. Res. Soc. Symp. Proc, **181** (1990) 597.
- [10] T. Arai, S. Yamagami, Y. Okuda, Y. Harada, Y. Miyamoto and K. Furuya, 2000 Topical Workshop on Heterostructure Microelectronics (TWHM '00), Tue-3, Kyoto, (2000).